Component-based Probabilistic Methodology for the Vulnerability Assessment of RC Frames Retrofitted with Dissipative Braces

F. Freddi & L. Ragni
Marche Polytechnic University, Italy

E. Tubaldi & A. Dall'Asta
University of Camerino, Italy

SUMMARY:
The paper illustrates a probabilistic methodology for assessing the vulnerability of low-ductility reinforced concrete (RC) buildings retrofitted by dissipative braces. The aim is to highlight the most important parameters controlling the capacity of these systems and specific aspects concerning the response uncertainties. The proposed methodology is based on local engineering demand parameters (EDPs) for monitoring the seismic response and on the development of component and system fragility curves before and after the retrofit. Its capability is tested considering a RC frame designed for gravity-loads only retrofitted by elasto-plastic dissipative braces. The results show the effectiveness of the methodology in describing the changes in the response and in the failure modalities due to the retrofit. Moreover, the retrofit effectiveness is evaluated by introducing proper synthetic parameters describing the fragility curves and highlighting the importance of employing local rather than global EDPs in the seismic risk evaluation of low-ductility frames.

Keywords: Reinforced Concrete Frame, Fragility, Vulnerability Assessment, Seismic retrofit, Dissipative Braces

1. INTRODUCTION

The damage occurred during recent earthquakes in many existing reinforced concrete (RC) buildings designed before the introduction of modern seismic codes has shown that these structures are very vulnerable to the seismic action due to their reduced ductility capacity. Thus, there is a significant need of modern retrofit techniques for increasing their safety and of reliable tools for assessing the effectiveness of the retrofit.

Among the various techniques currently employed for the retrofit, the use of dissipative braces appears to be very promising (Soong and Spencer 2002). These braces provide a supplemental path for the earthquake induced horizontal actions and thus enhance the seismic behavior of the frame by adding dissipation capacity and, in some cases, stiffness to the bare frame. It should be noted, however, that the introduction of a bracing system into a low-ductility frame often induces remarkable changes both in the collapse modalities and in the probabilistic properties of the seismic response of the structure. The latter aspect assumes a considerable importance in consequence of the high degree of uncertainty affecting the seismic input and of the differences in the propagation of this uncertainty through the two resisting systems (RC frame and dissipative bracing). For these reasons, the evaluation of the effectiveness of this type of retrofit technique in reducing the frame vulnerability should be performed within a probabilistic framework.

An increasingly popular approach for assessing in probabilistic terms the seismic vulnerability of structural systems and the effectiveness of a retrofit technique involves the development of fragility curves. These tools provide the probability of exceeding a specified limit state (LS) or failure condition, conditional to the strong-motion shaking severity, quantified by means of an appropriately selected intensity measure (*IM*). In this context, fragility curves are employed by Hueste and Bai 2006, Ramamoorthy et al. 2006, Güneyisi and Altay 2007, Özel and Güneyisi 2010. Although in these

studies probabilistic methodologies are employed for evaluating the effectiveness of different retrofit schemes, some modifications and extensions should be introduced in order to properly address the specific issues deriving from the use of dissipative braces for the retrofit of existing low-ductility RC frames.

The first issue is related to the choice of appropriate engineering demand parameters (EDPs) for monitoring the seismic response and evaluating the performance of the frame and of the retrofit system. In the studies listed above the fragility curves are developed by using the peak interstory drift as unique global EDP. This strategy is commonly pursued since monitoring the time-history of the local response of all structural members may be cumbersome, especially when complex models with a high number of degrees of freedoms are considered. In the cases of existing structures designed before the introduction of modern seismic codes, the relationships between local failure and global EDPs, such as the interstory drift, may change case by case, as demonstrated by the very different drift limits present in the literature (Hueste and Bai 2006, Ramamoorthy et al. 2006). Moreover, in existing structures retrofitted by means of dissipative braces, these relationships could change by increasing the dimension of the braces, due to the reduction of the flexural ductility capacity of the compressed columns involved in the bracing system. For these reasons, the use of global EDPs with code-specified limits is not recommended for the assessment of existing RC frames.

By contrast, the use of local component-specific EDPs (Lupoi et al. 2002), such as the strain demand at the most critical element sections or the shear demand on a beam-column joint, though more cumbersome, is not affected by the mentioned limitations. In addition, it permits to appropriately assess the probabilistic response of single resisting components (including the braces), their contribution to the system vulnerability, and the impact of the retrofit on the local response of the individual members (Padgett and Des Roches 2008).

A second relevant issue in defining a probabilistic methodology of analysis concerns the evaluation of the retrofit technique effectiveness, which is accomplished in the studies cited above by comparing the median values of the fragility curves of the structure before and after retrofit. This comparison has often implied the use of structural-independent *IM*s in past studies, such as the not very efficient peak ground acceleration (PGA). In fact, when the natural period of the bare frame differs from the natural period of the retrofitted frame, the comparison between fragility curves obtained by using more efficient structure-specific *IM*s (Katsanos et al. 2009) (e.g., the spectral acceleration at the fundamental period of the structure) would not directly provide information about the effectiveness of the retrofit (Liel et al. 2011). Furthermore, a more rational approach to accurately compute the changes in the safety margin due to retrofit should also account for the dispersion of the fragility curve, since this parameter affects the estimate of the seismic risk.

This paper proposes a fragility-based methodology aiming at overcoming the limits of the studies mentioned above. The methodology is developed by combining existing techniques already employed for different structural systems and by tailoring these techniques to the specific problem analyzed. Local EDPs are used to develop single component fragility curves while system fragility curves are derived and described by proper synthetic parameters suitable for use with any *IM*.

In the first part of the paper, the proposed methodology is accurately illustrated highlighting its advantages with respect to existing approaches. Then, its capability and effectiveness is tested by considering a realistic benchmark RC frame with limited ductility capacity. The frame is retrofitted by inserting a system of BRBs with elasto-plastic behavior designed for several levels of the base shear capacity. The braces are designed by applying a widespread method based on an equivalent single degree of freedom (SDOF) approximation (Soong and Spencer 2002). The application of the probabilistic methodology permits to evaluate the accuracy of the simplified design criterion and also to draw some important considerations about the behavior of the single resisting components, the effectiveness of the retrofit technique, and the structural safety increment.

2. PROBABILISTIC METHODOLOGY FOR VULNERABILITY ASSESSMENT

The seismic response of the frame before and after retrofit is affected by uncertainties in the earthquake input (record-to-record variability), in the properties of the system (model parameter uncertainty), and by lack of knowledge (epistemic uncertainty). The uncertainty affecting the earthquake input is taken into account by selecting a set of natural ground motion (g.m.) records that reflect the variability in duration, frequency content, and other characteristics of the input. The effects of model parameter uncertainty and epistemic uncertainty are usually less notable than the effects of record-to-record variability and they are not considered in this study (Kwon and Elnashai 2005).

In order to generate fragility curves, incremental dynamic analysis (IDA) (Vamvatsikos and Cornell 2002) is performed by subjecting the system to a set of selected g.m. records for increasing values of the seismic *IM*. The methodology proposed in this study is oriented to the use of structural-dependent *IM*s. In particular, the spectral acceleration $S_a(T)$ at the fundamental period of the structure T for a damping factor ξ=5% (Katsanos et al. 2009) is employed as *IM* due to its efficiency. This choice requires scaling the g.m. records in order to obtain the same value of $S_a(T)$ for the natural period of the structure, which is different for the bare and the retrofitted frames. IDA provides a set of samples of appropriately selected EDPs monitoring the system response for discrete values of the *IM*. As already discussed in the introduction, local EDPs, directly related to the component failure modes, are used in order to monitor the behavior of the most vulnerable system components and to capture the modifications to the frame response and collapse modalities induced by the introduction of the bracing system. The seismic demand on the frame elements (beams and columns) due to flexural moments and axial forces is controlled by monitoring the maximum-over-time values of the concrete compressive strain ε_c and of the steel strain ε_s at the most critical sections. The non-ductile mechanisms of the frames are controlled by recording the maximum-over-time values of the shear force V at the critical sections of each element of the frame, the diagonal tension stress σ_t, and the diagonal compression stress σ_c at each beam-column joint. Finally, in the retrofitted case, the seismic demand imposed on the retrofit system is controlled by evaluating the maximum-over-time value of a damage parameter i_d (e.g., the maximum-over-time value of the ductility demand μ_d for elasto-plastic braces) for each dissipative brace. The component fragility curves for the bare and the retrofitted frame are evaluated by considering the following limit states (LSs) chosen coherently with the monitored EDPs: LS1) ε_c exceeding the capacity limit ε_{cu} at each critical section, LS2) ε_s exceeding the capacity limit ε_{su} at each critical section, LS3) the shear demand V exceeding the shear resistance V_u at each critical section, LS4) σ_c exceeding the resistance in compression σ_{cu} at each joint, LS5) σ_t exceeding the resistance in tension σ_{tu} at each joint, and LS6) the damage index i_d overcoming the corresponding capacity i_{du} at each dissipative brace, (e.g., μ_d overcoming the limit μ_{du} for elasto-plastic braces).

The system fragility curves are then derived by assuming a series arrangement of the components, i.e., failure in one component yields system failure. The choice of the LSs and the series arrangement assumption is consistent with seismic code prescriptions requiring that all the considered LSs must be verified for all the structural members. Moreover, it allows of limiting structural damage on the existing frame, often sought by the retrofit criteria. However, it is noteworthy that the proposed methodology can be applied also with different assumptions on the system fragility curves. Finally, it is noted that the proposed methodology is purely numerical since it is based on the direct comparison between the samples of the demand and the corresponding capacity. Thus, the correlation among the various component LSs is automatically taken into account. The numerical fragility curves are approximated by analytical lognormal curves obtained through least-square minimization. The assumption of lognormality simplifies the analysis of the results and permits to synthetically describe the fragility of the systems by means of the two characteristic parameters. These are the median fragility capacity, $IM_{c,50}$, defined as the 50th fractile of the lognormal fragility curve and the logarithmic standard deviation or dispersion measure, β_c, given by:

$$\beta_c = \frac{1}{2}\ln\left(\frac{IM_{c,84}}{IM_{c,16}}\right) \tag{2.1}$$

where $IM_{c,84}$ and $IM_{c,16}$ are the *IM* values corresponding respectively to the 84th and the 16th fractile of the lognormal fragility curve, i.e., the values of the *IM* which yield failure respectively in 84 and 16 cases over 100. The use of lognormal fragility curves is very common and widely accepted in performance based earthquake engineering, since it permits to estimate the above defined parameters even when a limited number of EDP samples are available. Moreover, it permits to easily incorporate the effects of other sources of uncertainty in addition to the record-to-record variability, and it simplifies the evaluation of the seismic risk.

As already pointed out in the introduction, if a structural-dependent *IM* such as $S_a(T)$ is employed to monitor the seismic intensity, the comparison of the values of $IM_{c,50}$ obtained for the bare and retrofitted frame would not directly provide information about the effectiveness of the retrofit, since the natural period changes due to the retrofit. For this reason, the comparison should be performed between the values of the "capacity margin ratio" m_{50} (Liel et al. 2011), defined as the ratio between the value of $IM_{c,50}$ and the value of the *IM* corresponding to a reference return period, IM_{TR}. In the proposed methodology, IM_{TR} is assumed as the value of $S_a(T)$ for a reference return period such that m_{50}=1 for the bare frame, as illustrated in Fig. 2.1. By this way, the value of m_{50} obtained for the retrofitted frame directly measures the increment of seismic intensity that can be withstood by the retrofitted structure. In a similar way, based on the ratio $IM_{c,84}/ IM_{TR}$ and $IM_{c,16}/ IM_{TR}$, the factors m_{84} and m_{16} corresponding to the 84th and 16th fractiles of increment of capacity are defined. These parameters, together with parameter β_c, may also be used to assess in probabilistic terms the effectiveness of the retrofit, by accounting for the dispersion of the system response, which may have a non-negligible influence on the seismic risk assessment.

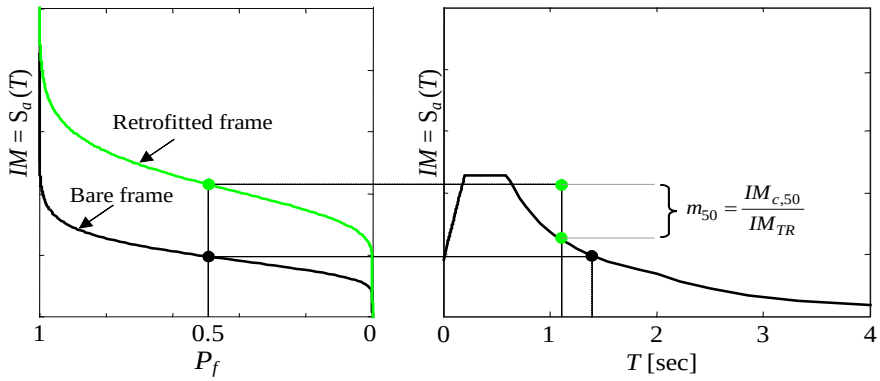

Figure 2.1. Definition of capacity margin ratio m_{50}: seismic fragility curves before and after retrofit (left), uniform hazard spectrum such that m_{50}=1 for the bare frame (right)

Finally, it should be noted that the proposed methodology permits to draw some important considerations regarding the performance of the system before and after the retrofit. In fact, by directly comparing the single component fragility curves to each other and to the system fragility curve, it is possible to evaluate the most vulnerable components and their contribution to the system vulnerability. This comparison permits to understand the changes in the response and in the failure modalities of the frame due to the retrofit.

3. RETROFITTING OF RC FRAME WITH ELASTO-PLASTIC BRACES

A three story RC moment resisting frame building is considered as case study. The building has been designed for gravity loads only and without any seismic detailing, applying the design rules existing before the introduction of modern seismic codes. The considered frame of the building is a three stories 3.66 m high and three bays, 5.49 m wide. Columns have a 300×300 mm^2 square section while beams are 230×460 mm^2 at each floor. Grade 40 steel (f_y = 276 MPa) and concrete with compression resistance f_c' = 24 MPa, were employed in the design. Fig. 3.1 shows the general layout of the structure and the position of the braces. The complete detailing may be found in Bracci et al. 1995.

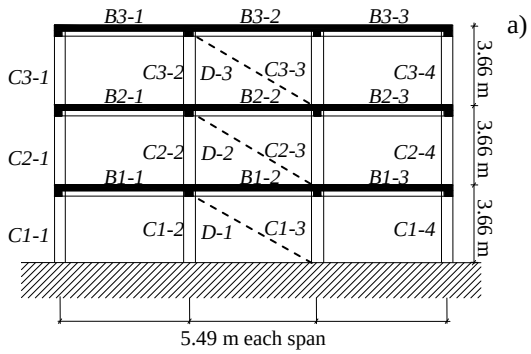

Figure 3.1. General layout of the structure and braces arrangement (adapted from Bracci et al. 1995)

A two-dimensional finite element (FE) model of the structure is developed in OpenSees (McKenna et al. 2006). Extended experimental results are available for a 1:3 reduced scale model of the frame and of its subassemblages (Bracci et al. 1995). The experimental information include the results of quasi-static lateral load tests of columns and beam-column joint subassemblages and shaking table tests of the whole frame. The FE model is validated by comparing the experimental results with the simulated test results of the 1:3 scale numerical FE models showing good agreement at global and local scale.

The retrofit design method is based on the pushover analysis of the existing frame under a distribution of forces corresponding to its first vibration mode. The stiffness of the dissipative braces is distributed at each story ensuring that the first modal shape of the bare frame remains unvaried after the retrofit. The strength distribution of the dissipative braces aims at obtaining simultaneous yielding of the devices at all the stories in order to maintain a similar deformation also in the post-elastic range. The interested reader is referred to Dall'Asta et al. 2009 for a more detailed description.

Fig. 3.2a shows the pushover curve obtained for the load distribution relative to the first vibration mode of the bare frame (mass participation factor of 86.4%). The ultimate capacity of the frame members is evaluated by considering the strain demand in the most critical concrete and steel fibres (ε_c and ε_s) and the corresponding limits ε_{cu} = 0.0035 and ε_{su} = 0.04 according to Eurocode 8. The other failure modes reported in Section 2 are not monitored in the application of the design procedure. The top story displacement d = 0.102 m denoting the failure of the most critical element (columns C1-2) is posed in evidence in Fig. 3.2a. It corresponds to a maximum interstory drift of about 1.0%, and to a base shear capacity V^i_f = 186 kN and it is assumed as the ultimate displacement d_u in the design procedure. Obviously, after this first failure, the bare frame still possess a residual capacity and can be pushed up to a top story displacement d = 0.183 m, at which all the base story columns fail (Fig. 3.2c).

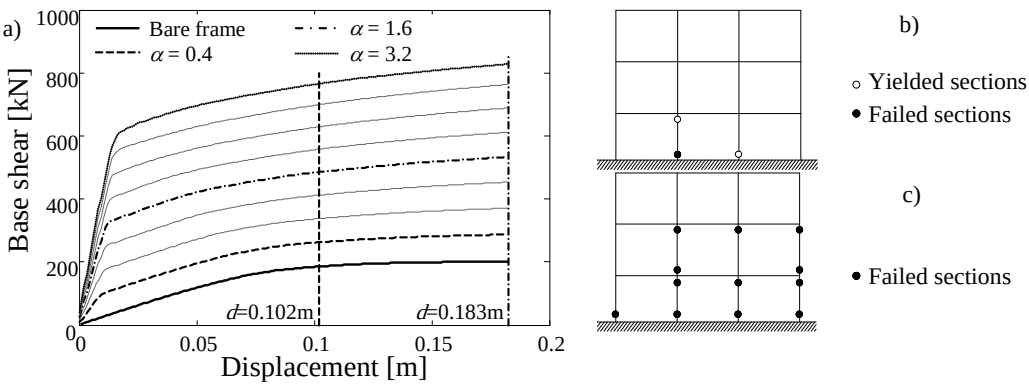

Figure 3.2. a) Pushover curves for bare and retrofitted frame, b) mapping of plastic hinges at d=0.102m , and c) mapping of plastic hinges at d=0.183m

The dissipative devices adopted in this case are BRBs typically described by an elasto-plastic behavior (Zona and Dall'Asta 2012). Differently from those commonly used in steel-structures, the dissipative

devices employed here are quite short, in order to obtain low yield displacements. Thus, the dissipative diagonal brace is made by assembling the BRB in series with an elastic brace characterized by an adequate over-strength. The ductility capacity μ_{0u} of the BRBs is assumed equal to 15, while the ductility capacity of the whole brace μ_{du} is assumed equal to 12 in order to obtain adequate dimension of the elastic braces. The bare frame is retrofitted by inserting a bracing system designed for several retrofit levels, measured by the ratio α between the base shear capacity of the bracing system V^1_d and that of the bare frame V^1_f. Parameter α assumes discrete values in the range from 0 (bare frame) to 3.2. Fig. 3.2a reports the pushover curves for all the α values. In Tab. 3.1, the axial yield force F^i_d and elastic stiffness K^i_d of the dissipative braces are given for three retrofit levels considered. Tab. 3.1 also reports the fundamental vibration periods for each retrofit level considered, calculated by considering an effective stiffness of the RC frame elements.

Table 3.1. Dissipative braces properties at each story

	α=0.4 (T=0.670 sec)		α=1.6 (T=0.404 sec)		α=3.2 (T=0.321 sec)	
Story	F^i_d [kN]	K^i_d [kN/m]	F^i_d [kN]	K^i_d [kN/m]	F^i_d [kN]	K^i_d [kN/m]
1	88	36046	351	144183	702	288365
2	75	25106	301	100423	601	200847
3	43	22921	173	91685	346	183371

4. VULNERABILITY ASSESSMENT

For the purpose of developing fragility curves, a number of 30 natural g.m. records are selected from the European database. These records are chosen in a range of magnitude and source to site distance of 5.5-7.0 and 25-75 km respectively and are compatible with the type 1 hazard spectrum given in Eurocode 8, with soil type D (S = 1.35) and peak ground acceleration a_g = 0.1Sg. In order to perform IDA, the records are scaled to the same value of the spectral acceleration at the fundamental vibration period of the system $S_a(T)$. It is noteworthy that the vibration period, and consequently the IM vary with α and thus, the g.m. records are re-scaled for each value of α.

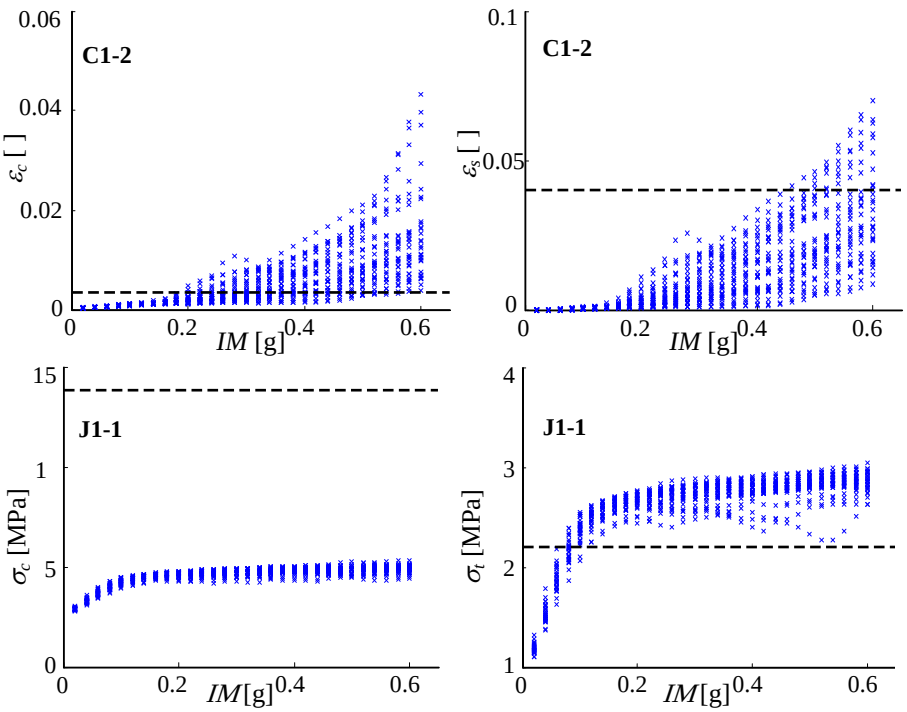

Figure 4.1. Demand samples and corresponding capacity limits for the case of bare frame

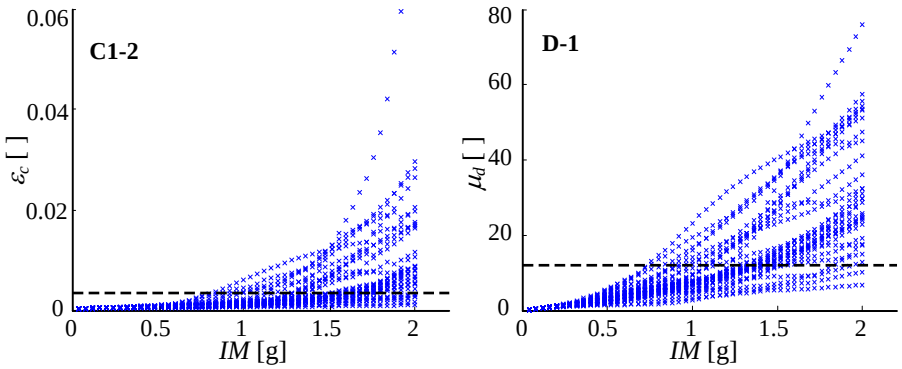

Figure 4.2. Demand samples and corresponding capacity limits for α=1.6

The dynamic analyses have been carried out on the numerical model developed in OpenSees and described in Section 3. For each record, for each *IM* value and for each element of the frame, the maximum-over-time values of the EDPs listed in Section 2 have been recorded. The maximum-over-time values of the tension (σ_t) and compression (σ_c) stresses and their capacity at each joints of the frame have been calculated through the formulas reported in Lupoi et al. 2002. Coherently with the capacity limits assumed in the retrofit design procedure, the limits of the concrete and steel capacity are set equal to ε_{cu} = 0.0035 and ε_{su} = 0.04, while the elements shear resistance V_u is evaluated according to the formulas reported in Lupoi et al. 2002. Fig. 4.1 and Fig. 4.2 report the results of IDA, expressed in terms of variation with *IM* of the monitored EDP samples and their capacity.

In Fig. 4.1, the samples of the maximum-over-time values of the concrete compressive strain ε_c and steel strain ε_s at the most critical section of C1-2 are illustrated, for the case of the bare frame. The corresponding capacity limits are also reported. In the same figure, the values of σ_c and σ_t recorded at joint J1-1 are also reported and compared with the corresponding capacity limits. Fig. 4.2 plots the values of ε_c at column C1-2 and the maximum-over-time value of the ductility μ_d experienced by dissipative brace D-1 at the base story, for the case of retrofitted frame with retrofit level α=1.6.

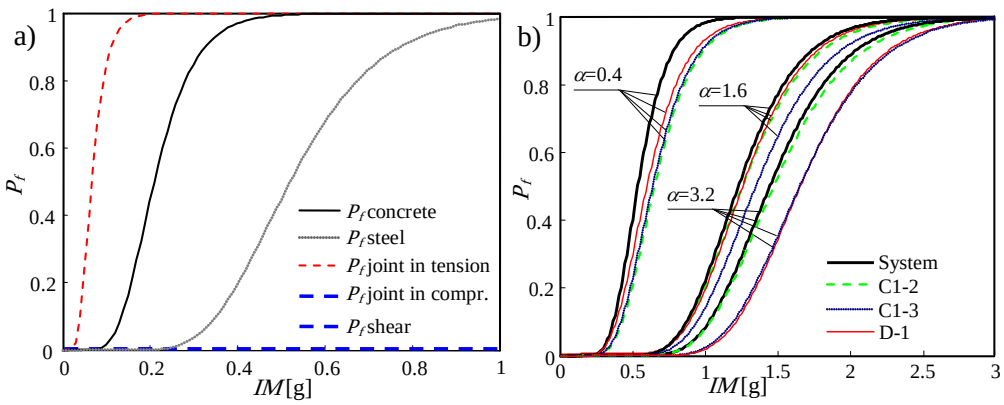

Figure 4.3. a) Lognormal fragility curves for the different failure modes and b) Fragility curve of the system and of the most vulnerable components for three retrofitted cases.

The component fragility curves are evaluated for each LS and for each frame member by comparing the demand samples with the corresponding capacity limits. Then, the system fragility curves are derived by assuming a series arrangement of the component fragilities. Fig. 4.3a reports the lognormal component fragility curves for the case of the bare frame. It is observed that joint failure in tension is the most critical LS. However, this LS provides only a measure of the damage of the joints due to the concrete degradation and it is not deemed as critical as the brittle failure of the joint in compression. Hence, it is disregarded in developing the system fragility curve and therefore concrete crushing in compression (LS1) is the most critical failure modality, while steel rupture (LS2) is much less

probable and failure of joints in compression and shear failure have a zero probability of occurrence.

Fig. 4.3b shows the fragility curves of the most vulnerable elements and of the system for three retrofitting levels corresponding to α=0.4, α=1.6 and α=3.2. The most vulnerable components of the bare frame are column C1-2 and C1-3, failing in concrete crushing mode (LS1) and exhibiting a similar vulnerability. For α=0.4 the vulnerabilities of the two columns remain comparable to each others, and also similar to the vulnerability of the most critical dissipative brace (D-1). This confirms the reliability of the simplified design procedure, which has the two main aims of avoiding drastic changes to the internal action distribution in the frame and of achieving a simultaneous failure of both the frame and the braces. Also in the case corresponding to α=1.6, the fragility curves of the most critical frame components and of the most critical dissipative brace are very close. However, column C1-2 is more vulnerable than C1-3. This can be attributed to the bracing system configuration, which induces a higher axial load on column C1-2 with respect to C1-3. The trend is confirmed by the results of the case corresponding to α=3.2, where the fragility curve of column C1-2 differs significantly from the others and tends to coincide with the system fragility curve. This means that system failure is mainly due to C1-2 column failure, as consequence of the excessive axial force transmitted by the bracing system on this column.

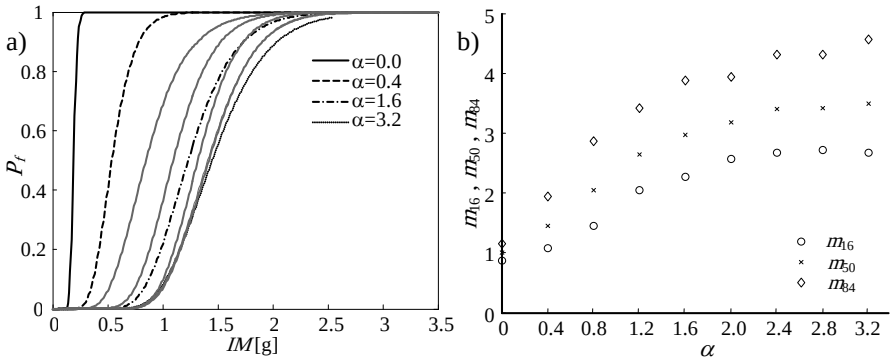

Figure 4.4. a) System fragility curves for the bare frame and for the retrofitted frame, and b) variation with α of the factors m_{50}, m_{84} and m_{16}.

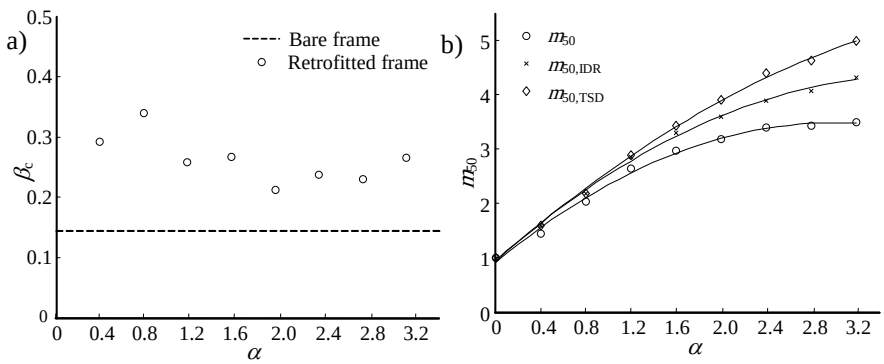

Figure 4.5. Variation with α of a) dispersion measure β_c and b) factor m_{50} corresponding to the use of different local and global EDPs.

Fig. 4.4a compares the system fragility curves for all the retrofit levels considered. Parameter $IM_{c,50}$ increases for increasing values of α, as expected. However, as already stressed previously, this parameter does not directly provide information about the effectiveness of the retrofit, since the natural periods of the systems are different. Fig. 4.4b reports the factors m_{50}, m_{84}, and m_{16}, which have been defined in Section 2 in order to compare the retrofit effectiveness when a structural dependent *IM* is used. It is observed that for values of α up to 1.6, the capacity margin ratio increases about linearly with α, while for higher values this relation becomes strongly non-linear. This implies that the

effectiveness of the retrofit increases weakly for values of α larger than 1.6, in consequence of the premature failure of column C1-2 mainly due to the high axial forces induced by the braces.

Fig. 4.5a plots the dispersion measure β_c evaluated according to Eqn. 2.1 for increasing values of α and shows that a significant increase of the dispersion occurs when elasto-plastic braces are introduced into the bare frame. This is consequence of the increase of the number of the vulnerable components (frame members and dissipative braces) and of the more pronounced nonlinear behavior induced by the introduction of BRBs. Accounting for this increase of dispersion is important due to its influence on the estimate of the seismic risk.

Finally, in order to quantify the differences in the retrofit effectiveness evaluation when local and global EDPs are used, system fragility curves are evaluated also by considering global EDPs, such as the maximum interstory drift (IDR) and the top story drift (TSD). Fig. 4.5b reports the comparison between the values of previously defined parameter m_{50} and the values of parameters $m_{50,\mathrm{IDR}}$ and $m_{50,\mathrm{TSD}}$ evaluated on the basis of the fragility curves developed by considering the IDR and the TSD respectively.
In order to make this comparison, the global EDPs limits $\mathrm{IDR_u}$ and $\mathrm{TSD_u}$ are chosen so that $IM_{c,50} = IM_{c,50;\mathrm{IDR}}$ ($m_{50,\mathrm{IDR}}$=1) and $IM_{c,50} = IM_{c,50;\mathrm{TSD}}$ ($m_{50,\mathrm{TSD}}$=1) for the case of bare frame. The limits obtained are $\mathrm{IDR_u}$= 1.302% and $\mathrm{TSD_u}$= 1.029%. It is evident from Fig. 4.8b that the use of global EDPs instead of more accurate local EDPs results in a significant overestimation of the seismic increment capacity of the retrofitted frames, especially for large α values. In fact, as already discussed in the introduction, local phenomena such as the increment of axial force in the columns adjacent to the dissipative braces are not accounted for by these global EDPs. This confirms that local EDPs must be adopted to accurately estimate the effectiveness of the retrofit based on dissipative braces. Otherwise, if global EDPs are considered, proper limits need to be estimated for each retrofit level.

4. CONCLUSIONS

The paper illustrates a probabilistic methodology for assessing the vulnerability of RC buildings with limited ductility capacity and the effectiveness of the retrofit by means of dissipative braces. The methodology is based on the development of fragility curves of the bare and the retrofitted frames. It employs an efficient structure-dependent intensity measure (*IM)* and involves performing non linear IDA to account for the randomness of the earthquake excitation. Local EDPs are used to capture the modifications of the frame response induced by the introduction of the bracing system. Numerical fragility curves are derived by comparing the samples of the demand with the corresponding capacity limits. The component fragility curves are built for each single structural component and for each single LS considered. The system fragility curves are derived by assuming a series arrangement of the component LSs. Finally, proper synthetic parameters describing the system fragility curves are introduced in order to accurately compute the increment in the safety achieved by the retrofit while employing a structure dependent *IM*, such as the spectral intensity at the natural period of the structure.

The capability and effectiveness of the proposed methodology is tested by considering a realistic benchmark RC frame with limited ductility capacity retrofitted by elasto-plastic braces. The braces are designed by applying a widespread method based on an equivalent nonlinear SDOF approximation and by considering different values of the shear capacity of the bracing system. On the basis of the analysis of the results, the following conclusions can be drawn. The comparison of the single components fragility curves permits to individuate the most vulnerable elements of the frame that may change by increasing the retrofit level. In the case study considered, these elements coincide with the two columns involved in the bracing system, failing in concrete crushing mode. However, for low retrofit levels, the fragility curves of these columns are very similar to each other and they are also similar to the fragility curve of the most critical dissipative brace, whereas for large retrofit levels the fragility curve of the most compressed column significantly differs from the other fragility curves and tends to coincide with the system fragility curves. This is a consequence of the very different axial

load induced in the columns by the braces action in the case of high retrofit level.

In order to compute accurately the increment of capacity due to retrofit for increasing values of α (retrofit levels) while using a structure-dependent *IM*, parameter m_{50} is introduced. The values assumed by m_{50} for all the retrofit cases considered demonstrate that the effectiveness of the retrofit system increases only weakly for high retrofit levels in consequence of the previously described variations in the component vulnerability. Moreover, the response dispersion, evaluated by means of parameter β_c, significantly increases when elasto-plastic braces are introduced into the bare frame. This result is important since the seismic risk estimate is strongly affected by the dispersion of the system response. Finally, the capacity margin ratio evaluated by using local EDPs for monitoring the system response is compared with the capacity margin ratios evaluated by monitoring the response through global EDPs such as the maximum interstory drift and the top story drift. The results obtained show that the use of these global EDPs results in a significant overestimation of the seismic increment capacity due to dissipative braces action, especially for large retrofit levels. Thus, it is concluded that the accurate estimation of the effectiveness of the retrofit by means of dissipative braces should be carried out by employing local EDPs capable of accounting for local phenomena.

REFERENCES

Bracci, J.M., Reinhorn, A.M., Mander, J.B. (1995). Seismic resistance of reinforced concrete frame structures designed for gravity loads: performance of structural system. *ACI Structural Journal.* **92:5**,597-608.

Dall'Asta, A., Ragni, L., Tubaldi, E., Freddi, F. (2009). Design methods for existing RC frames equipped with elasto-plastic or viscoelastic dissipative braces. *Proceedings of XIII National Conference ANIDIS*.

Freddi, F. (2012). Local engineering demand parameters for seismic risk evaluation of low ductility reinforced concrete buildings. *Ph.D. Thesis, Polytechnic University of Marche*.

Güneyisi, E.M., Altay, G. (2008). Seismic fragility assessment of effectiveness of viscous dampers in R/C buildings under scenario earthquakes. *Structural Safety.* **30:5**,461-480.

Hueste, M.D., Bai, J.W. (2006). Seismic Retrofit of a Reinforced Concrete Flat-Slab Structure: Part II - Seismic Fragility Analysis. *Engineering Structures.* **29:6**,1178-1188.

Katsanos, E.I., Sextos, A.G., Manolis, G.D. (2009). Selection of earthquake ground motion records: A state-of-the-art review from a structural engineering perspective. *Soil Dynamics and Earthquake Engineering.* **30:4**,157-169.

Kwon, O.S., Elnashai, A. (2006). The effect of material and ground motion uncertainty on the seismic vulnerability curves of RC structure. *Engineering Structures.* **28:2**,289-303.

Liel, A.B., Haselton, C.B., Deierlein, G.G. (2011). Seismic Collapse Safety of Reinforced Concrete Buildings: II. Comparative Assessment of Non-Ductile and Ductile Moment Frames, *Journal of Structural Engineering.* **137:4**,492-502.

Lupoi, G., Lupoi, A., Pinto, P.E. (2002). Seismic risk assessment of rc structures with the “2000 SAC/FEMA" method. *Journal of Earthquake Engineering.* **6:4**,499-512.

McKenna, F., Fenves, G.L., Scott, M.H. (2006). OpenSees: Open system for earthquake engineering simulation. Pacific Earthquake Engineering Center, University of California, Berkeley, CA.

Özel, A.E., Güneyisi, E.M. (2011). Effects of eccentric steel bracing systems on seismic fragility curves of mid-rise r/c buildings: a case study. *Structural Safety.* **33:1**,82-95.

Padgett, J.E., Des Roches, R. (2008). Methodology for the development of analytical fragility curves for retrofitted bridges. *Earthquake Engineering and Structural Dynamics.* **37:8**,1157-1174.

Ramamoorthy, S., Gardoni, P., Bracci, J. (2006). Probabilistic Demand Models and Fragility Curves for Reinforced Concrete Frames. *Journal of Structural Engineering.* **132:10**,1563-1572.

Soong, T.T., Spencer, B.F. (2002). Supplemental energy dissipation: state-of-the-art and state-of-the-practice. *Engineering Structures.* **24:3**,243-259.

Vamvatsikos, D., Cornell, C.A. (2002). Incremental dynamic analysis. *Earthquake Engineering and Structural Dynamics.* **31:3**,491-514.

Zona, A., Dall’Asta, A. (2012). Elastoplastic model for steel buckling restrained braces. *Journal of Constructional Steel Research*. **68:1**,118-125